Chapter 11
The Multiscale Architectures of Fish Bone and Tessellated Cartilage and Their Relation to Function

Ronald Seidel, Aravind K. Jayasankar, Ron Shahar and Mason N. Dean

Abstract When describing the architecture and ultrastructure of animal skeletons, introductory biology, anatomy and histology textbooks typically focus on the few bone and cartilage types prevalent in humans. In reality, cartilage and bone are far more diverse in the animal kingdom, particularly within fishes, where cartilage and bone types exist that are characterized by features that are anomalous or even pathological in human skeletons. Here, we discuss the curious and complex architectures of fish bone and shark and ray cartilage, highlighting similarities and differences with their mammalian skeletal tissue counterparts. By synthesizing older anatomical literature with recent high-resolution structural and materials characterization work, we frame emerging pictures of form-function relationships in these tissues and of the evolution and true diversity of cartilage and bone.

11.1 Introduction

A major innovation in vertebrate evolution was the emergence of calcium phosphate-based mineralized tissues, which enabled the evolution of a diversity of protective armors, teeth and an internal skeleton [1–3]. Mineralized skeletons first appeared in

R. Seidel · A. K. Jayasankar · M. N. Dean (✉)
Department of Biomaterials, Max Planck Institute of Colloids and Interfaces,
14424 Potsdam, Germany
e-mail: Mason.Dean@mpikg.mpg.de

R. Seidel
e-mail: Ronald.Seidel@mpikg.mpg.de

A. K. Jayasankar
e-mail: Aravind.Jayasankar@mpikg.mpg.de

R. Shahar
The Robert H. Smith Faculty of Agriculture, Food and Environmental Sciences,
Koret School of Veterinary Medicine, The Hebrew University of Jerusalem, PO Box 12,
76100 Rehovot, Israel
e-mail: Ron.Shahar1@mail.huji.ac.il

Y. Estrin et al. (eds.), *Architectured Materials in Nature and Engineering*, Springer Series in Materials Science 282,
https://doi.org/10.1007/978-3-030-11942-3_11

fishes, some 500 million years ago, as dermal exoskeletons covering the bodies of basal jawless fishes. This outer bony armor was lost in evolution and later supplanted by the internal skeletons we know from modern species that, for the most part, are either entirely bony (as in the vast majority of vertebrates) or consist of a cartilaginous core stiffened by a mineralized collar (as in sharks and rays, the "cartilaginous fishes") [1, 4, 5].

Regardless of whether the primary skeletal tissue type is mineralized cartilage or bone, all vertebrate mineralized tissues are comprised of water, non-collagenous proteins, and collagen fibrils mineralized with carbonated apatite (e.g. [6]). The range of material properties observed in vertebrate skeletal tissues are therefore not determined by changes in chemistry (e.g. by introducing heavy metals, as in some invertebrate tissues) (e.g. [7]), but rather through variation in the proportions of the building blocks—proteins, mineral and water—and in the architectures of the tissues [6, 8]. The bulk mineral content of mammalian bone, for example, ranges from ~50% to nearly 100% ash content (from antler to beaked whale rostrum, respectively), resulting in large variations in stiffness and toughness [9].

The natural diversity of mammalian bone has made it a particularly useful system for studying the effects of composition and structure on mineralized tissue material properties. There are bone tissues with extremely high or low bulk mineral densities (e.g. otic vs. antler bone); bone tissue with similar bulk mineral density, but drastically different ultrastructure or mesostructure (e.g. osteonal vs. fibrolamellar and cortical vs. cancellous bone, respectively); and bone tissue with local variation of both composition and structure (e.g. cortical bone with fiber-lamellar and osteonal regions) (see review in [10]). Studies of these tissues have informed our understanding of structural and compositional complexity in bony skeletons, however, have focused predominantly on a small fraction of mammalian species, thereby largely ignoring the wide range of habitat, bone, and skeletal tissue types of the rest of vertebrates.

To understand the true scope of variation of vertebrate skeletal tissues, with regard to structure, composition, and mechanics, it is important to look beyond the limited number of the often-used model species and sample vertebrates as broadly as possible. By examining evolutionary alternatives to mammalian bone, we can expand and reframe our understanding of form-function relationships in vertebrate skeletal tissues and the factors that drove their evolution. Here, we discuss the two major mineralized tissue types of fishes: the bone of bony fishes and the tessellated cartilage of sharks and rays (Fig. 11.1). These tissues are comprised of the same basic components as the bone in mammalian skeletons, but exhibit distinct 'mesostructural' tissue arrangements that result in distinctive mechanical properties. Furthermore, as fishes occupy a huge range of habitats and ecological niches, exhibit extensive morphological diversity, and represent at least 55% of all vertebrate species, they

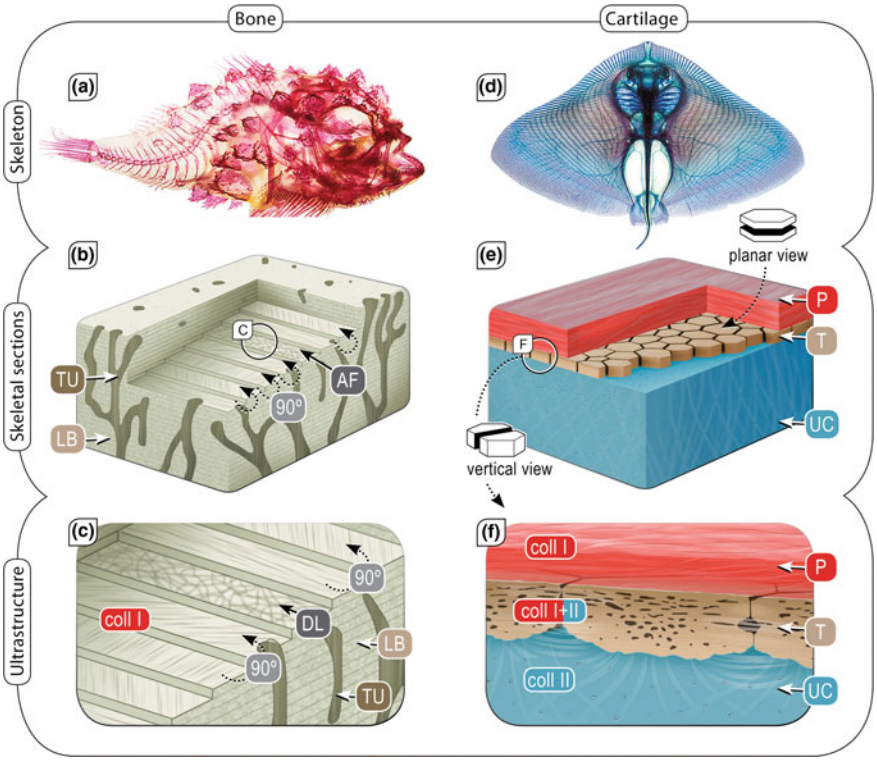

Fig. 11.1 General organization of the two primary mineralized skeletal tissues in fish. (**a–c** Bony fish bone; **d–f** Shark and ray tessellated cartilage) Detailed descriptions of the two tissue types are provided later in text. **a** Cleared and stained bony fish skeleton (lumpsucker, *Eumicrotremus orbis*). **b–c** Fish bone, depending on the species, is either osteocytic or anosteocytic, with perforating tubules, and exhibiting a laminated tissue organization. Each layer is patterned on fibers, smoothly and gradationally spiraled from layer to layer (plywood-like structure) until a turn of 180° is reached, and a layer of anisotropically oriented fibers (AF) is incorporated. **d** Cleared and stained butterfly ray skeleton (*Gymnura* sp.). Specimen is young and not yet fully mineralized: blue color shows the cartilage of the skeleton, which will form a mineralized layer later in life. **e**, **f** Structure of tessellated cartilage of sharks and rays, comprising mineralized tiles (tesserae) covering the skeletal cartilage. Abbr.: DL = disordered layer; coll = collagen; LB = layered bone; P = Perichondrium; T = Tesserae; TU = Tubules; UC = uncalcified cartilage. Images in **a** and **d** courtesy of A. Summers

offer unparalleled opportunity for defining and understanding the parameter space of form-function relationships in vertebrate skeletal tissues. The study of structure-function relationships in fish skeletal tissues is still incipient: this chapter aims to describe the current understanding of fish skeletal tissue architecture, drawing on recent high-resolution ultrastructural data, and discussing potential links between these features and available mechanics data.

11.2 Fish Osteocytic and Anosteocytic Bone

Both cartilaginous fishes (Chondrichthyes) and bony fishes (Osteichthyes) evolved from jawless fish ancestors, the earliest vertebrates appearing some 500 million years ago. The superclass Osteichthyes, which is the largest group of vertebrates in terms of species numbers, evolved in two parallel lines, namely the lobe-finned fishes (Sarcopterygii, to which mammals also belong), and the ray-finned fishes (Actinopterygii). Fishes from both of these groups possess mineralized internal skeletons consisting of an exceptionally large number of articulating bones in comparison with mammals, particularly in the cranium.

From a material perspective, the bones of all bony vertebrates consist of the same four basic building blocks: type-I collagen fibrils, carbonated calcium apatite, water and a small amount of non-collagenous proteins (NCPs). These building blocks are extremely similar among the different phyla, both in terms of their chemistry and geometric size. For example, small angle x-ray scattering studies performed on bone samples obtained from several fish and mammalian species revealed that the mineral platelets of fish and mammalian bone are comparable in terms of thickness, degree of orientation and length ([11, 12]; personal observations). The organic phase of fish bone (mostly type-I collagen) was shown to be identical to that of mammals as well [13].

Across vertebrates, bone is a dynamic living tissue, which typically contains three types of cells: osteoblasts (bone forming cells), osteoclasts (bone resorbing cells) and osteocytes (osteoblasts trapped within the matrix they produced). These cells provide bones with their active metabolism and the ability to adapt their structure and composition to changing loading circumstances (a process called modeling). In addition, bone cells allow for continual renewal of the tissue, by replacing packets of old bone with new and flawless material (remodeling). Modeling and remodeling are carried out by the coordinated activity of osteoclasts and osteoblasts, and are believed to be regulated by the osteocytes, perhaps by responding to changes in fluid flow in the lacuna-canalicular network and/or local bone strains [10, 14, 15].

Although the cellular and matrix components of the bones of the fish skeleton are largely similar to those of other vertebrates (Fig. 11.2a–f), two remarkable observations, made already 150 years ago, delineated drastic differences. Firstly, it was found that the bones of a substantial number of fish species—more than half of the several tens of thousands of fish species [16]—do not contain osteocytes (i.e. are anosteocytic), although they do contain osteoblasts and osteoclasts (Fig. 11.2g–i). Secondly, it was observed that anosteocytic bone occurs predominantly in the advanced teleosts, whereas the bones of the basal teleosts are typically osteocytic [17]. This observation suggests that osteocytes were effectively lost during the evolution of the bony fish lineage and therefore that the anosteocytic state represents a functional advantage of some sort to the fish skeleton, although the nature of this advantage is still unclear.

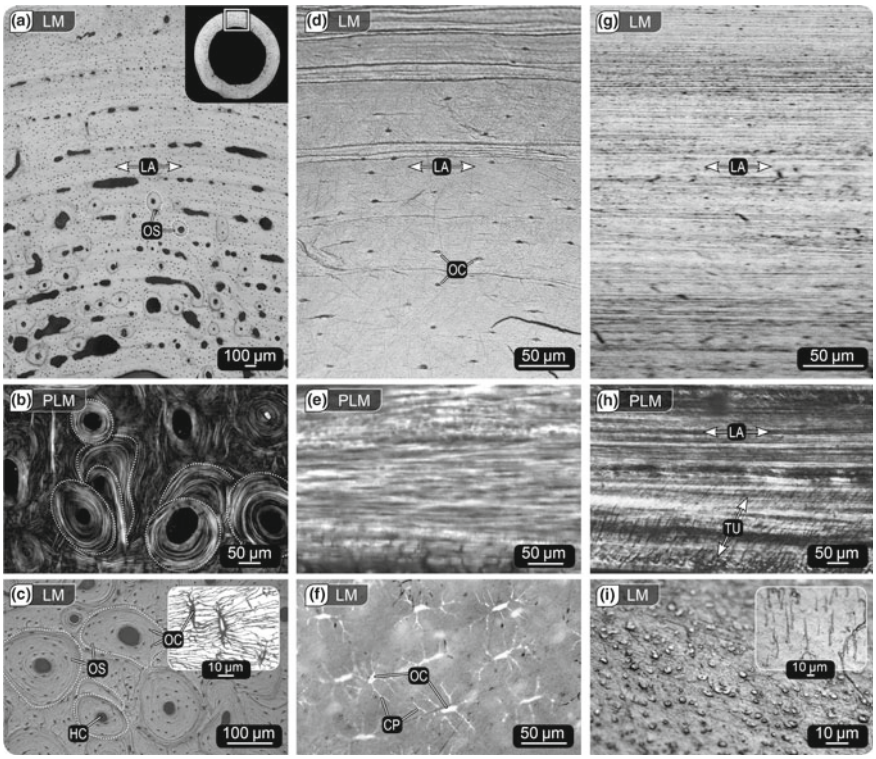

Fig. 11.2 Ultrastructural differences of vertebrate bone types. (**a**–**c** mammalian bone; **d**–**f** fish osteocytic bone; **g**–**i**: fish anosteocytic bone). **a** Cross-section of a mammalian tibia exhibiting a lamellar appearance with multiple primary osteons. **b** Secondary osteons under polarized light, their overlapping indicating bone remodeling. **c** Light microscopy image of secondary osteons, showing their central Haversian canals, which contain blood vessels and nerves, and are surrounded by concentric lamellae. Osteocytic lacunae can be seen within the lamellae, with small canaliculi connecting each lacuna to its neighbors, together forming the lacuna-canalicular network. **d**–**f** Osteocytic bone from carp (*Cyprinus carpio*) and **g**–**i** anosteocytic bone from tilapia (*Oreochromis aureus*) have a similar lamellar appearance, but the latter bone type lacks the osteocytes present in the osteocytic carp bone (shown in **f**). Tubules (**h**) perforate the lamellae of both fish bone types. Abbr.: CP = cell processes; HC = Haversian canal; LA = Laminae/Layers; LS = Lacunar spaces; OC = Osteocytes; OS = Osteon; TU = Tubules. Image in **c** courtesy of A. Roschger

Of particular interest is how advanced fish can maintain the health of their bones and avoid failure without having osteocytes. The belief that osteocytes are vital to bone health and mutability is a central paradigm in bone biology [10, 18] and argues that bone without osteocytes will be unable to model and remodel, and will therefore frequently fail disastrously. This is supported by studies showing that the removal of osteocytes has a detrimental effect on bone health and material properties (reviewed in [10]). And yet, the anosteocytic bone of neoteleost fish is not only an extremely common bone type—there are likely 16,000 species of anosteocytic fishes—but also

the skeletons of neoteleost fishes perform their mechanical function for very long times without failure (some fish have life expectancies of more than 100 years [19]).

The predominant lack of osteocytes among fishes can have several possible explanations. One possibility is that osteocytes do not perform the functions we have assigned to them, at least not exclusively, and the regulation of modeling and remodeling can be accomplished without the need for osteocytes. Another (even more intriguing) possibility is that the structural features of anosteocytic bone material are such that modeling and remodeling are not required for the tissue's health. This could mean, for example, that anosteocytic bone material is inherently highly resistant to crack initiation and/or crack propagation. We discuss below several recently characterized structural features that appear to be unique to fish bone and that may play some role in mediating interesting material properties of the tissue.

Although many fish species lack a fundamental cellular component of bone (osteocytes), the bone matrices of both anosteocytic and osteocytic fish species typically exhibit a lamellar structure, a basic meso-scale structural motif shared with the bone of all other vertebrates. In both mammals and fishes, lamellae are typically <7 μm thick, consist of mineralized collagen fibrils (~100 nm in diameter) and ground substance (water and non-collagenous proteins), and form strata in the bone tissue that are visible in various forms of microscopy. In cross sections of mammalian long bones, for example, lamellae may form concentric rings surrounding the entire interior marrow cavity (Fig. 11.2a), or form smaller structural units (osteons) surrounding blood vessels [10]. Osteons are structural results of remodeling of the bone matrix (renovation of small regions) and can be packed in high densities (20–70 osteons/mm^2, [20]), especially in heavily remodeled tissues, and as a result can impart a striking structural patterning to mammalian bone (Fig. 11.2b, c) [10]. In contrast, fish bone was long described as being largely featureless in appearance, due to its often simple layered structure and comparative rarity of vasculature (Fig. 11.2d, g) [21]. The layered appearance of most fish bone (both osteocytic and anosteocytic) results from its formation process, where new lamellae are deposited upon older ones throughout the fish's life [21].

The recent use of modern structural and material analysis techniques, however, has shown that fish bone is in fact characterized by a wide array of rather complex architectural features, some of which are not seen in mammalian bone. These include hyperostoses (non-pathological, spherical bone growths attached to fin elements), acellular osteon-like structures, and porous feather- or honeycomb-like bone tissue morphologies (Fig. 11.3) (reviewed in [10, 21]). Modern characterization advances have also revealed nanostructural aspects distinct to fish bone lamellae. A recent study used serial surface view, focused ion beam milling—SSV FIB-SEM, a technique combining ablation of thin layers (5–15 nm thickness) and serial, high resolution imaging—to characterize the 3D arrangement of collagen fibrils at the nanometer scale in the anosteocytic opercular (gill cover) bone of tilapia (*Oreochromis aureus*), and compare it to the collagenous architecture of several types of mammalian cortical bone [21]. In mammals, bone lamellae are comprised of sub-lamellar layers that vary in their spatial arrangement, degree of order (co-alignment of fibers) and fiber directionality according to species and taxon [22]. The analysis of the anosteocytic

fish bone lamellae revealed some similarity to mammalian bone in being comprised of planar sub-lamellar layers of mineralized collagen fibrils [21]. However, whereas mammalian bone seems to involve complicated interweavings of ordered and disordered sub-lamellar layers (the latter containing the cells and their processes), the lamellae of the anosteocytic fish bone exhibited a conceptually simpler arrangement. Fibrils in the sub-lamellar layers smoothly and gradationally spiraled from layer to layer, resulting in a layered plywood-like structure (Figs. 11.1a–c and 11.4a). When the sequence of fibril orientations completed a rotation of 180°, a thin layer of poorly-oriented fibrils intervened before the next spiral of sub-lamellar layers. As the bones of only a tiny fraction of existing fish species have been examined at this level of detail to date, it remains unclear how universal this 'lamellated bone' motif is among fishes and whether it is linked to the distinct mechanical properties of fish bone (see below).

In addition to the basic layered structure of fish bone, over the last 150 years several authors have noted the presence of micron-sized tubules within the bulk of the bone, in some cases present in very high densities [17, 23–28]. The nature of these tubules (e.g. their content and function) were not clear, and led to several contradictory speculations, positing that the tubules either contained unmineralized collagen fibrils, or sensory extensions of surface osteoblasts, or even osteocytes (i.e. contradicting the axiom that advanced teleost bone lacks osteocytes). The FIB-SEM study by Atkins and colleagues [21] confirmed the presence of these tubules, but also enabled the characterization of their contents and structure at high resolution and in three dimensions. The tubules were shown to form an intricate 3D array, with each 1–4 μm diameter tubule containing a bundle of tightly-packed hypo-mineralized collagen fibrils. The tubules were oriented mostly orthogonal to the lamellar plane (Fig. 11.4b–d), suggesting that they, and the internal fibers, are linking bone lamellae, in a manner analogous to Coptic bookbinding where pages are sewn together with thread. It is reasonable to assume that they serve a mechanical purpose, such as pinning together the bone layers and resisting shear failure, although this remains to be shown. They may also perhaps be associated with a sensory function, given that the tubules extend so deeply into the bone tissue and could somehow monitor the strains experienced within the bulk of the bone material.

The unique structural features of fish bone and the possibility that these affect an inherent failure resistance offer a strong motivation for the study of fish bone material, in particular its mechanical properties and behavior. Nevertheless, the mechanical properties of fish bone (and particularly anosteocytic bone) have received far less attention than those of the bones of tetrapods, especially mammals. Limited available data suggest that fish bone is much more compliant than tetrapod bone, having an elastic modulus of 5–8 GPa [17]. This is less than half of typical mammalian cortical bone stiffness in the principal direction (axial orientation of the long bones ~15–25 GPa [8]). In contrast, in post-yield mechanical testing, fish bone was observed to be considerably tougher than mammalian bone (can absorb much more energy before failure), with strains at failure often exceeding 5%, approximately two times the failure strains commonly seen in mammalian bone (Fig. 11.5a). Since fish bone consists of the same basic building blocks as tetrapod bone (mineralized

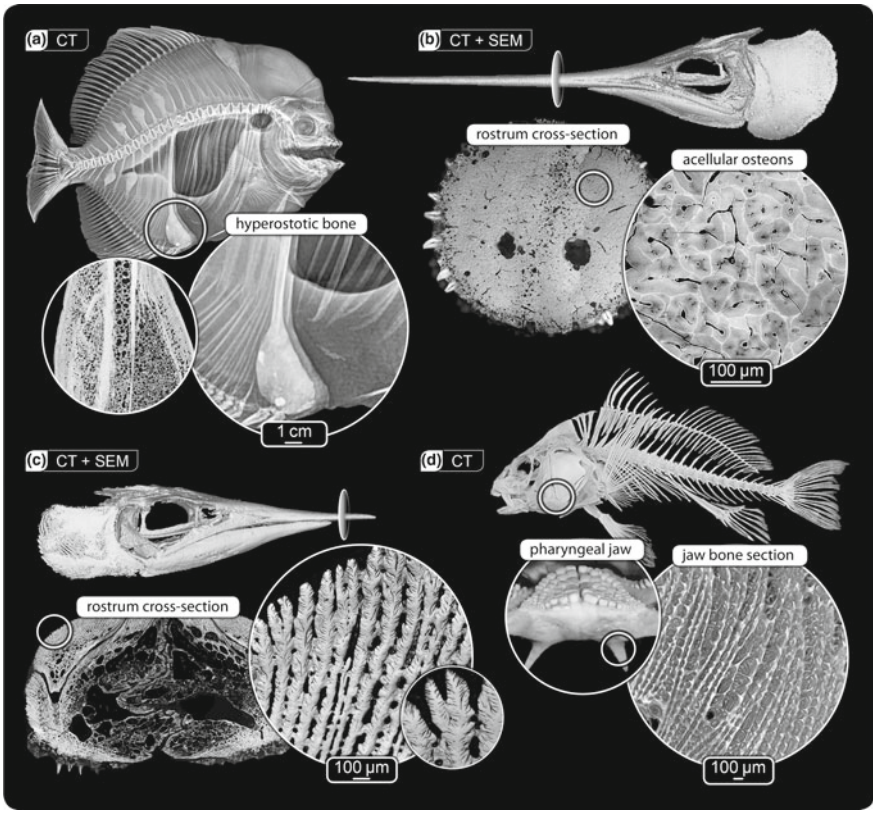

Fig. 11.3 Variation in fish bone ultrastructure. CT scan, light microscopy and backscatter SEM images of non-lamellar fish bone: **a** hyperostotic bone in longfin spadefish (*Platax teira*), **b** acellular osteons in the rostrum of blue marlin (*Makaira nigricans*), **c** feather-like bone in the rostrum of shortbill spearfish (*Tetrapturus angustirostris*) and **d** honeycomb-like organization of bone in the pharyngeal jaw of black drum (*Pogonias cromis*). Modified with permission from [64], copyright John Wiley Sons, Inc.

collagen fibrils and water), the mechanical data suggest that some features of the 3D structural arrangement of fish bone and its mineral density are responsible for its unusual mechanical behavior. We hypothesize that the mineral density of anosteocytic fish bone and its unique tubules-linking-lamellae ('bookbinding') structure are responsible for these unusual mechanical properties (e.g. that post-yield deformation is controlled and fracture is arrested by the hypo-mineralized tubular fiber bundles). Deeper investigation of the mechanical properties of fish bone, particularly post-yield behaviors and fracture toughness according to different load axes, will help to establish the structural roots of this tissue's impressive resistance to failure.

An additional and particularly intriguing observation about fish bones concerns the effect of wetting dry samples, or *vice versa*. All biological tissues are affected

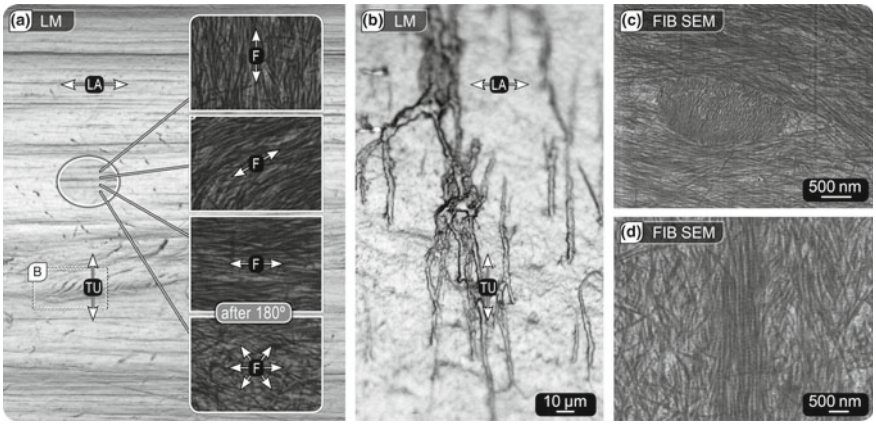

Fig. 11.4 Fibrous organization and tubules in acellular fish bone (*Oreochromis aureus* operculum). **a** In successive tissue lamellae of fish bone, the predominant fiber orientation is rotated, with a layer of random fiber orientation intervening after the fiber orientation has rotated 180°. **b–d** Tubules run perpendicular to and perforate the lamellae; in FIB-SEM images hypomineralized fiber bundles are visible within the tubules (**c** Tubule cross-section; **d** Tubule longitudinal section). Abbr.: F = Collagenous fibers; LA = Laminae/Layers; TU = Tubules

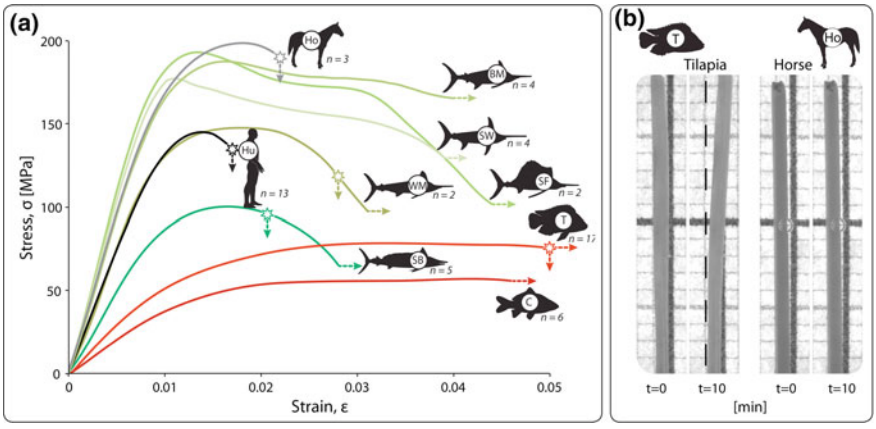

Fig. 11.5 Variation in structure-function relationships in vertebrate bones. **a** Stress-strain curves of bone beams from mammal and fish species tested in three-point bending; the initial slope is the stiffness, regions after the initial peak represent post-yield deformation, and stars indicate the average fracture strain for those samples fractured during testing. Lines lacking stars bent without failure until the displacement limit of the testing machine was reached. Note the high toughness (large post-yield region) of fish bone and combination of high stiffness and high toughness of billfish bones, relative to human and horse bone. Modified from [18], copyright 2014 National Academy of Sciences. **b** Comparison of the behavior of hydrated tilapia and horse bone beams (t = 0) following dehydration (t = 10 min); the large deflection of tilapia bone is reversible with rehydration

structurally and mechanically when they change from a wet to a dry state. This change is usually quite subtle in mineralized materials, involving only a slight deformation of tissue samples. However, we have observed, using samples from a variety of species, that this change can be quite dramatic in fish bone. For example, results of a test comparing beams of identical dimensions made of equine cortical bone and *Oreochromis aureus* (tilapia) opercular bone illustrate this difference: when hydrated equine beams were dried they deformed only slightly, whereas when hydrated beams of anosteocytic fish bone were dried they exhibited pronounced bending and some torsion (Fig. 11.5b). This transformation was completely reversible upon re-hydration in beams from both species. We postulate that the cause for the pronounced effect of wetting and drying on fish bone samples results from their unique 3D architecture and structural arrangements of the tubular hypo-mineralized and tightly-packed collagen bundles linking adjacent bone laminae (Fig. 11.4b–d), and we are currently investigating the phenomenon and its mechanics further.

11.3 Shark and Ray Tessellated Cartilage

11.3.1 Structure

Sharks and rays are often referred to as the 'cartilaginous fishes', indicating what sets the skeletons of these fishes apart from the bony skeletons of the vast majority of other vertebrates. Like most vertebrates, sharks and rays develop an embryonic unmineralized cartilage skeleton; however, this is never replaced by bone during ontogeny, and instead remains mostly cartilaginous throughout their lifetime (Fig. 11.1d–f). Bone and unmineralized cartilage are clearly quite different materials for building skeletons, exhibiting major differences in: (1) tissue organization (bone and cartilage are patterned on type-I and type-2 collagen, respectively); (2) material properties (bone is about 10,000 times stiffer than cartilage in most physiological loading regimes); and (3) response to tissue damage (unlike bone, cartilage has a limited vascular and neural supply and can't heal) [8, 29, 30].

We believe the distinct structural patterning of shark and ray skeletons allows the cartilage to perform many of the same mechanical roles that bone performs in the other 98% of vertebrates: each piece of the cartilaginous endoskeleton is covered in a thin layer of thousands of mineralized, polygonal tiles called tesserae, typically hundreds of microns wide and deep [4, 31, 32] (Fig. 11.6). This tessellated crust of mineralized tissue is sandwiched between the unmineralized cartilage core of the skeleton and an outer fibrous perichondrium wrapping each skeletal element, resulting in a layered fibro-mineral composite. This unique endoskeletal tiling typically occupies only 30% or less of each skeletal element by volume [33], yet appears to be an important evolutionary innovation of elasmobranch fishes. Tesserae have characterized elasmobranch skeletons for more than 400 million years [34] and are vital to shark and ray skeletal biology. Tesserae not only permit interstitial growth

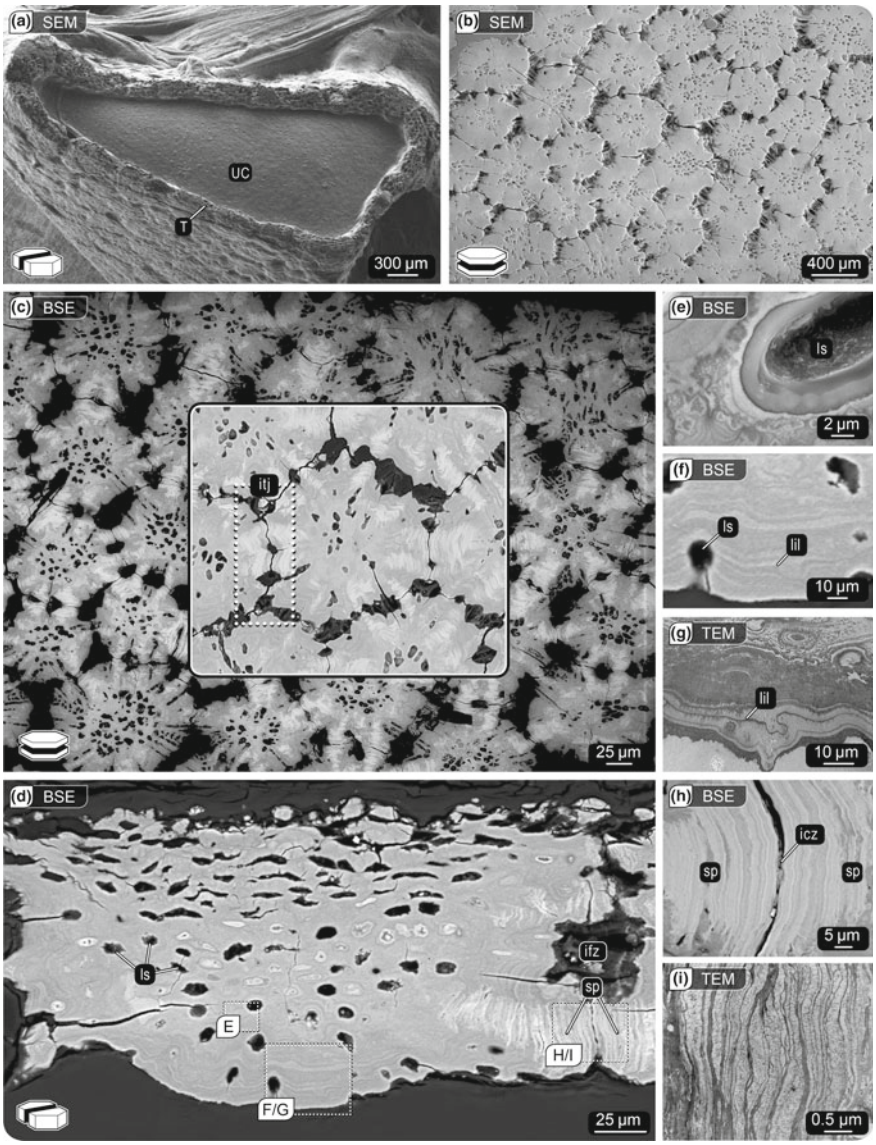

of the mineralized layer—via deposition of new mineral at the margins of tesserae [4, 31, 35], a growth mechanism impossible with a continuously mineralized crust that cannot remodel—but also afford stiffness to skeletal elements (see Sect. 11.3.2 below).

◂**Fig. 11.6 Tessellated cartilage of elasmobranch fish (sharks and rays)**. Note icons showing section orientation, introduced in Fig. 11.1. **a** Cryo-electron microscopy image of an elasmobranch skeletal piece in cross-section showing the unmineralized cartilage core (*UC*) sheathed in a thin layer of mineralized tiles, called tesserae (*T*). **b**, **c** Planar and **d** vertical views of the tesseral layer, showing abutting tesserae from an adult specimen (**b** SEM; **c**, **d** backscatter SEM imaging, showing only mineralized tissue), revealing the variation in the shapes of tesserae and their intertesseral joints (comprised of regions of direct contact and gaps of fibrous connection between tesserae; see Fig. 11.7). Note the regional variation in cell lacunae shape and in gray value within tesserae in **b**, reflecting local differences in mineral density and showing regions of high mineralization associated with zones of intertesseral contact. The most prominent, diagnostic features of tesserae are magnified in **e**–**i** using backscatter and transmission electron microscopy, showing **e** filigree mineralization pattern surrounding a lacuna, **f**, **g** Liesegang lines of accretive growth and **h, i** the laminated, hypermineralized 'spokes' reinforcing intertesseral contact zones. All samples from the round stingray, *Urobatis halleri*. Abbr.: ICZ = intertesseral contact zone; IFZ = intertesseral fibrous zones; ITJ = intertesseral joint; LIL = Liesegang lines; LS = lacunar space; SP = spokes

The dogfish *Scyliorhynus canicula* and round stingray *Urobatis halleri* are the best-studied elasmobranch species as far as the general development and ultrastructure of the tessellated endoskeleton are concerned (e.g. [4, 31, 33, 36–38]). During development, tesserae first appear in the embryonic skeleton as isolated platelets of cartilage calcification, embedded in and separated by unmineralized cartilage. The individual tiles grow by mineral accretion on their existing surfaces, a process reflected in periodic, concentric layers of varying mineral density (Liesegang lines) in the mineralized tissue [4, 32, 33] (Fig. 11.6d–g). This accretionary growth eventually brings young tesserae into contact with one another at their lateral edges. Once this occurs, pronounced high mineral density features, known as 'spokes', develop at the regions of direct contact of two adjacent tesserae (Fig. 11.6d, h, i). Spokes are laminated structures, comprised of densely packed layers of oscillating mineral density, stacked parallel to intertesseral contact surfaces. As the animal and its skeleton grow, tesserae continue to enlarge by accretion, spokes lengthen, radiating outward from tesseral centers like spokes on a wheel (Fig. 11.6c). The growth mechanisms behind the striking repeated structural pattern in spokes are unknown, but the association of spokes with zones of intertesseral contact argues that the mechanical interaction of tesserae may be a guiding factor.

Both Liesegang lines and spokes illustrate that tesserae are more than simply homogeneous mineralized blocks, instead having local mineral density variation as heterogeneous as that seen in bone [4, 10]. Unlike mammalian bone, however, there is no evidence of remodeling or repair in tesserae [4, 29, 33]. If tessellated cartilage—which apparently performs many of the same functional roles as bone—truly is a deposition-only tissue with no healing capacity, it may also possess in-built strategies for avoiding catastrophic damage, similar to the neoteleost bone described in the previous section. This is an enticing suggestion of the potential for tessellated cartilage as an inspiration for manmade design, since the mechanical performance of the tissue might be reproducible by mimicking structural and material properties, rather than biological action (e.g. cellular involvement, tissue remodeling).

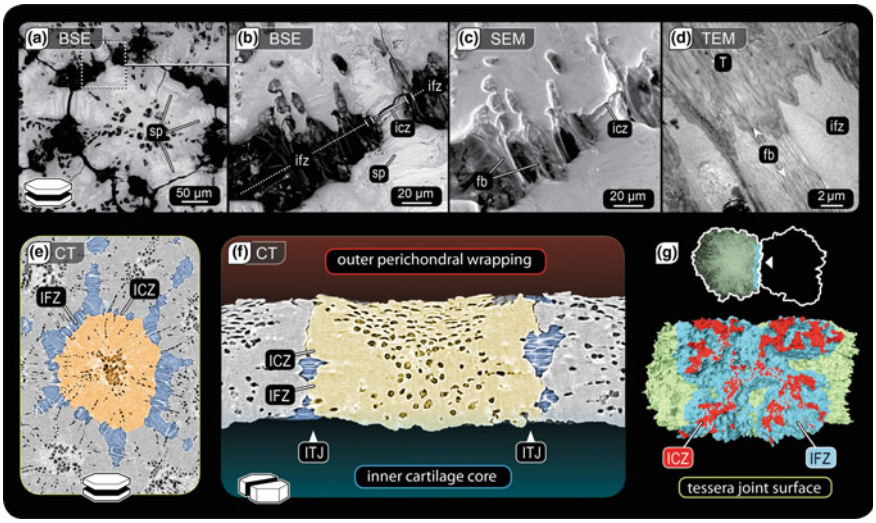

Fig. 11.7 Flexible linkage of tesserae—collagen fibers at the intertesseral joints. **a**–**d** Backscatter SEM, environmental SEM and TEM images showing the structural complexity of a joint of two abutting tesserae in planar section: **a**, **b** joints are comprised of regions where tesserae are in direct contact (*ICZ*) and gaps (*IFZ*) filled with cells and densely aligned fiber bundles (*fb*) linking adjacent tesserae. **e**–**g** High-resolution synchrotron μCT scans show no macroscopic tesseral overlapping or interdigitation, but fibrous and contact zones interact in complex ways as illustrated in **g** viewed from the perspective of the neighboring tessera. See abbreviations in previous figure

Our understanding of the features driving tessellated cartilage mechanical properties are in their infancy, but the tissue's performance appears to hinge to a large degree on the interactions and spatial arrangements of softer and harder materials (Fig. 11.7). There is some evidence, for example, that the serial laminae in spokes, by possessing differing mineral densities, introduce interfaces to redirect cracks and dissipate their energy [4]. At a larger scale, the interactions between tesserae are also characterized by material heterogeneities: the sides of tesserae exhibit smooth patches where they come in direct contact with their neighbors, but these are surrounded by regions of densely aligned collagenous fibers, tethering the tesserae together [4, 33] (Fig. 11.7a–d). The bipartite nature of intertesseral joints is thought to impart an interesting mechanical anisotropy to the skeleton as a whole, providing stiffness or flexibility to the tessellated composite layer, depending on the loading conditions. However, these interactions have never been expressly visualized, largely due to technical challenges of visualizing movements of small features in 3D, at adequate resolution and in hydrated conditions. Recent high-resolution synchrotron micro-CT (Fig. 11.7e–g) and modeling studies of tessellated cartilage (see below) are making headway overcoming these difficulties.

The general structural features and tissue arrangements of tessellated cartilage described above appear to be largely universal for sharks and rays [4]. Our high-resolution electron microscopy and synchrotron tomography data, however, indicate

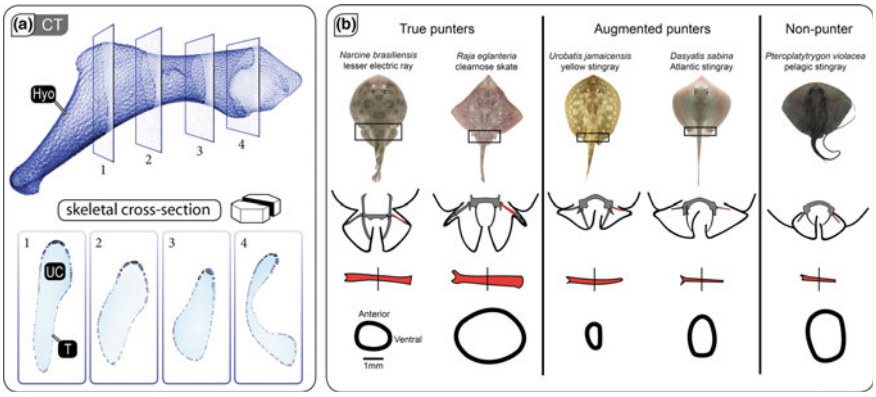

Fig. 11.8 Local variation in tesserae form and suggested relationship to function. **a** Micro-computed tomography of a stingray hyomandibula (*Hyo*; skeletal piece connecting the jaws with the skull), virtually sectioned in 4 different anatomical positions, showing thicker tesserae (T) in convex regions. Abbr: UC = unmineralized cartilage. **b** Cross-sections of pelvic propterygia (skeletal piece supporting the pelvic fins) from different species, showing cross-sectional shape variation according to the species' reliance on 'punting' behavior (use of pelvic fins to move along the sea floor). Modified with permission from [35], copyright Company of Biologists Ltd.

that the shape and structure of tesserae can vary, both within individuals (e.g. between different regions of the skeleton) and among species, in ways that further suggest that the interactions between tesserae are functionally important. For example, the tesserae of different shark and ray species have been shown to vary enormously in size (from <100 μm to nearly 1 mm in width and thickness) and shape, ranging from disc-like plates to cuboid blocks [4, 34, 39]. The shapes of tesserae also appear to vary according to their location on a skeletal element (e.g. depending on the skeleton's local surface curvature; [4, 40]) and according to the skeletal element they cover (e.g. consistently cuboid in the rostral cartilages of some sharks and specific regions of the jaws of some rays; [34, 39]) (Fig. 11.8a). These observations are strongly suggestive of a form-function relationship between the shape of tesserae, their joints and the effective mechanical behavior of the tesseral mat and whole skeletal elements, but these links are only beginning to be established.

11.3.2 Mechanics

In general, the study of tessellated cartilage mechanics lags far behind the study of skeletal anatomy and tesseral ultrastructure. However, the results of several works, taken together, begin to paint a picture of how the structural and mechanical properties of elasmobranch cartilage interrelate and how tesserae play an important role in tailoring skeletal properties to specific ecological roles and high load-bearing activities.

An understanding of the global mechanical properties of tessellated cartilage—a composite with relatively discrete material phases—demands characterization of the properties of the primary tissue constituents: uncalcified cartilage, unmineralized joint fibers and mineralized tissue. Capturing *in vivo* properties, however, is complicated by the fine scale 3D structural arrangements of tessellated cartilage and the need for testing conditions that mimic physiological conditions (e.g. hydration and load rates). Available evidence indicates that elasmobranch uncalcified cartilage has a proteoglycan and collagen content similar to mammalian hyaline cartilage and suggests that it can be at least as stiff, if not several orders of magnitude stiffer for similar loading rates (mammalian: 0.45–19 MPa vs. elasmobranch: 2–775 MPa—[41–43]. These properties depend apparently on the species and the skeletal element tested; more rigorous studies are required to understand the relationships between mechanical properties and composition, loading rate and phylogeny.

Whereas covering a cartilage-like gel with a hard, continuous shell is expected to increase the stiffness but decrease the flexibility of a composite, there is some indication—from tessellated cartilage, but also fabricated arrays (e.g. [44])—that a tessellated shell with interacting tiles can be a 'best of both worlds' configuration, maximizing desirable properties of both tissue phases. Fahle and Thomason [45] showed that compared with embryonic (non-tessellated) small-spotted catsharks (*S. canicula*), adult individuals have jaw cartilage that has a higher ability to damp mechanical energy, but is also stiffer. A large portion of the stiffness is surely due to the tessellated layer in adult animals [4, 31, 37, 46]. From the biological perspective, this change in properties permits adults to consume harder prey than newborns [45], but is also particularly intriguing for engineering considerations since stiffness and damping are typically negatively correlated in manmade materials.

The arrangement of the tessellated layer relative to the direction of loading plays a considerable role in elasmobranch skeletal tissue mechanics. Tessellated cartilage cubes from blue sharks (*Prionace glauca*) loaded normal to the tesseral mat (in stress relaxation experiments) behaved similarly to non-tessellated cubes, being ~45 times softer than tessellated cubes with the load applied in-plane with the tesseral mat [42] (Fig. 11.9). These results are supported by indentation experiments performed on hydrated jaw samples from two large sharks (*Carcharodon carcharias*, *Carcharias leucas*) [47]. Nanoindentation experiments typically involve pushing a very small, hard tip (e.g. with a tip radius of hundreds of nanometers) into a material to examine hardness and elastic modulus at very small scales. However, as the indenter used by Ferrara et al. was very large (100 μm) and approached the dimensions of some tesserae [4, 31, 48], we believe their data are more representative of the properties of the composite material (e.g. tesserae and their surrounding soft tissues), in that they report values considerably softer than either the tesserae themselves [42, 49] or whole skeletal elements [35]. Deeper investigation into the relationship between local properties and emergent skeletal properties is required to untangle the contradictions in available data.

Variations around the generalized tessellated cartilage anatomy described above, when interpreted in the context of animal ecology, also provide perspectives on *in vivo* skeletal performance, as well as the functional limits of the tissues. For

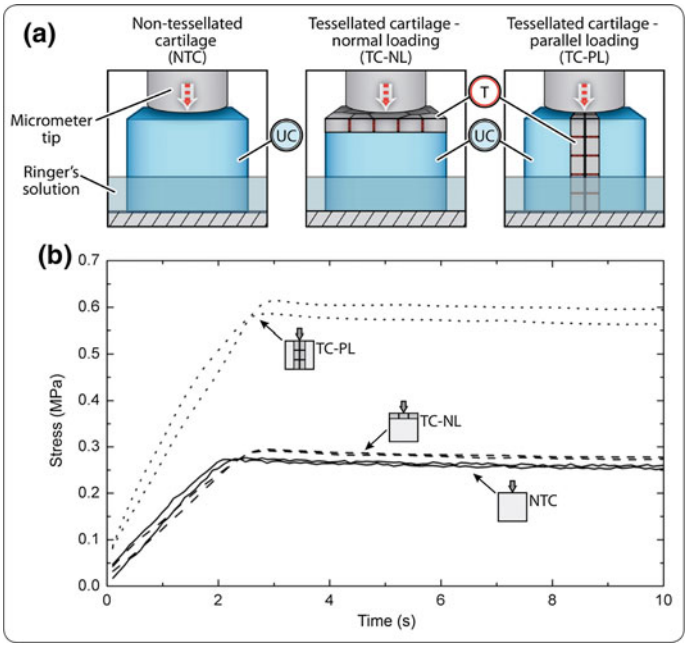

Fig. 11.9 Contribution of the tesseral layer and its orientation to mechanical properties. Stress relaxation behavior of blue shark (*Prionace glauca*) cartilage was tested either with tesserae (T) oriented normal (*TC-NL*) or parallel (*TC-PL*) to the loading direction, or without tesserae (*NTC*). Stress relaxation behavior of non-tessellated cartilage (*NTC*) and tessellated cartilage under normal loading (*TC-NL*) were similar, but the behavior of tessellated cartilage samples under parallel loading (*TC-PL*) was far stiffer, indicating that the performance of tessellated cartilage is strongly dependent on the orientation of loads relative to the tesseral layer. Modified with permission from [42], copyright 2014 Elsevier

example, in addition to the outer tessellated layer, the jaws of many batoid fishes (rays and relatives) contain hollow tessellated struts (trabeculae), typically hundreds of microns in diameter, spanning the uncalcified cartilage-filled lumen of the jaws [50–52] (Fig. 11.10a). These appear to be arranged along lines of principal loading, often in narrow regions of the jaws or jaw joints (e.g. [51, 53]), and are therefore structurally and functionally convergent with the trabecular bone found in tetrapods. The importance of trabeculae to the reinforcement of tessellated cartilage is underlined by the high density of trabeculae in the jaws of species that experience high skeletal loads during feeding, such as the lesser electric ray which uses explosive jaw protrusion to retrieve buried prey [50] or myliobatid stingrays which employ high bite forces to crush hard shelled mollusks ([51, 52, 54]; see also Fig. 1 in [55]).

Additional mechanisms described for reinforcing tessellated cartilage against bending involve either thickening of the skeleton's hard, outer cortex (i.e. the tesseral layer) or modifications to the cross-sectional shape of skeletal elements. In the former, the tesseral layer is often locally thickened (e.g. the tesserae in skeletal cross-sections

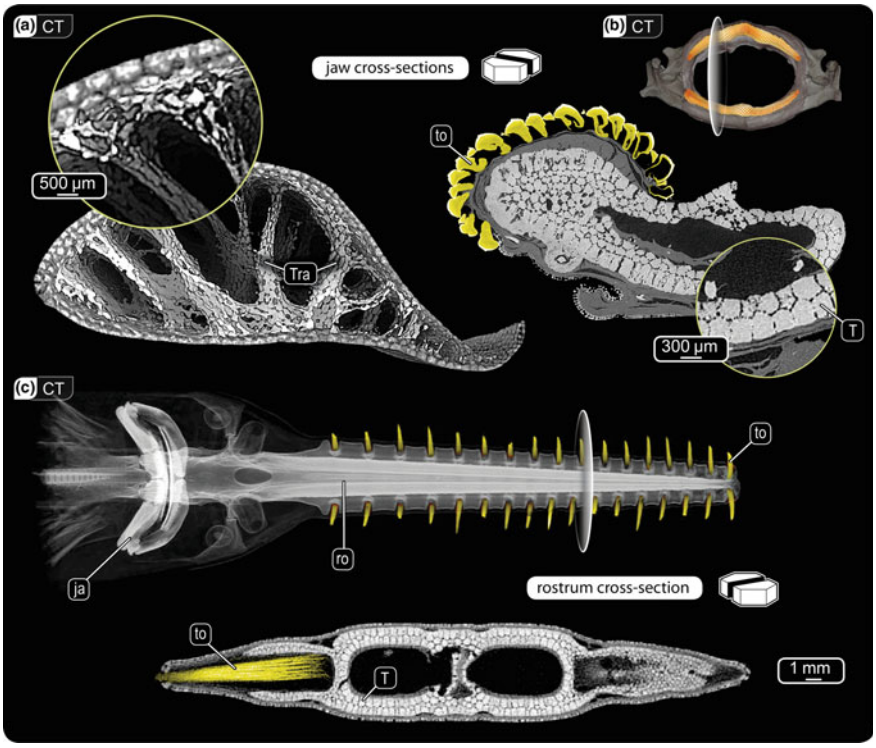

Fig. 11.10 Methods of reinforcement of tessellated cartilage. All images are volume renderings or virtual cross-sections of micro-CT scans. **a** Cross-section of the jaws of the cownose ray (*Rhinoptera bonasus*), a hard prey specialist, showing mineralized trabeculae (struts) running through the jaw, reinforcing the primary biting direction. Alternatively, tessellated cartilage can be reinforced by multiple tesseral layers, as in **a** the outer layers of the cownose ray jaw, **b** the jaws of a wedgefish (*Rhynchobatus* sp.) and in **c** the rostral 'saw' of a sawfish (*Pristis microdon*). Abbr: JA = jaws; RO = rostrum; T = tesserae; Tra = Trabeculae; To = Tooth

in Fig. 2 of [4] vary up to 4× in thickness), particularly in regions in line with principal loading or in areas of high curvature [4, 40, 53, 56–58]. The cortex can also be thickened via introduction of additional tesseral layers, particularly in the jaws of large carnivorous sharks [59], the "saws" of sawfish [33, 51], or the jaws of species with diets containing large proportions of hard shelled prey (Fig. 11.10b, c) [52, 55]. Up to 10 supernumerary tesseral layers have been recorded in the jaws of some extant species [57]. High flexural stiffness in whole skeletal elements appears to result from either high mineral content (a proxy for the proportion of tesserae in an element or cross-section), skeletal cross-sectional shapes with high second moment of area or combinations of the two [35, 56, 58, 60]. Skeletal element flexural stiffness has also been shown to be correlated with differences in ecology—for example, supporting specific locomotion [35, 60] or feeding modes [56]—but mineral content and cross-sectional shape/size do not always vary predictably (e.g. animals with large

skeletal cross-sections can have either very high or very low mineral content [35, 56, 58]) (Fig. 11.8b). This indicates that tessellated cartilage has evolved to be 'modular', where functionally and ecologically relevant skeletal mechanical properties can be achieved through a variety of structural mechanisms (e.g. cortical thickening, increased second moment of area, introduction of trabeculae), rather than compositional alterations to the apatite mineral in the tessellated layer (e.g. the introduction of heavier elements as can occur in invertebrate tissues [7].

The mechanical influence of the *tessellation* itself—the tiling of the cortex and the varying patterns formed by tesserae—has yet to be investigated in situ, likely due to the experimental difficulties posed by the size of tesserae and their complex

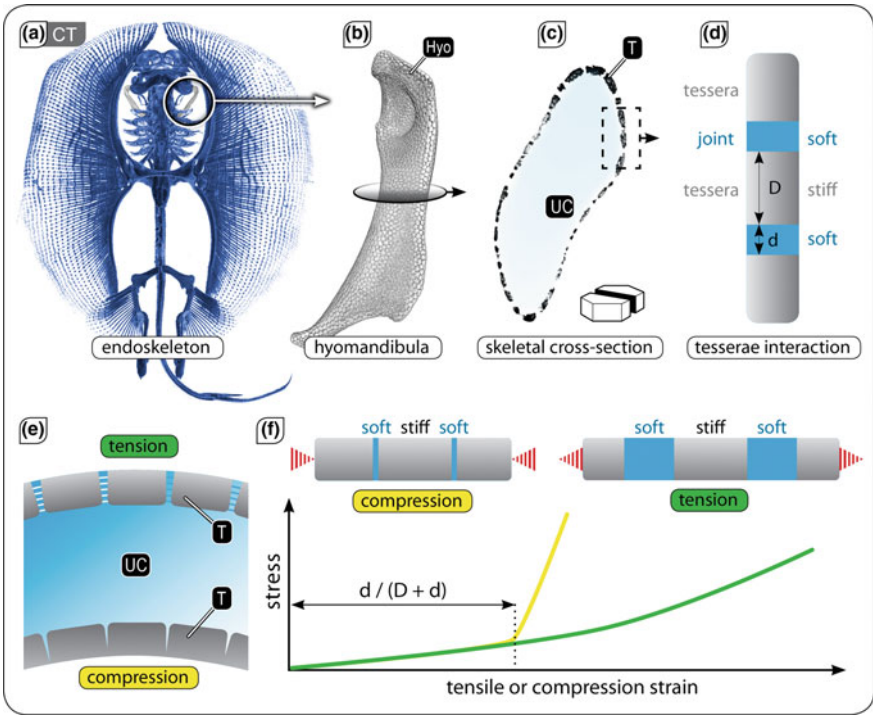

Fig. 11.11 Proposed compression-tension asymmetry in tessellated cartilage. **a–c** Micro-CT scans of the skeleton and hyomandibula (Hyo) of a stingray (*Urobatis halleri*) illustrating the composite nature of tessellated cartilage, formed by stiff mineralized tiles (T) separated by softer unmineralized joints. Abbr: UC = unmineralized cartilage. **d** Schematic of alternating soft and hard constituents in a tessellated system. **e** Schematic section of tessellated skeletal element in bending, with the top and bottom tessellated layers experiencing tension and compression, respectively. **f** Hypothetical stress-strain curves illustrating the proposed tension-compression asymmetry of a tessellation. In tension, the deformation will be dominated by the stretching of the soft joint interlayer (yellow line), whereas in compression, the behavior is stiffer (green line), dominated by the stiff tiles colliding once the thickness of the soft interlayer is exhausted [at a compressive strain of approximately d/(D + d)]. Modified from [61]

tissue connections. Several studies, however, have incorporated existing materials and/or structural data from the biological tissue in computational simulations and mathematical models of tessellated cartilage, helping to shape informed and testable hypotheses relating to tissue growth and mechanics. Empirical models of tessellated cartilage cross sections, for example, based on biological material and ultrastructural data, suggest that the tessellation plays a role in controlling the stress distribution within the skeletal tissue during bending [61, 62]. This is a function of the narrow joints between tesserae, the structure of which is hypothesized to result in strikingly different properties in tension than compression (Fig. 11.11). In a hypothetical laminated tessellated cartilage beam—a monolithic core of unmineralized cartilage sandwiched between two thin tessellated layers—subjected to bending, the tesserae on the side of the beam loaded in tension should pull apart from one another, whereas tesserae on the compressive side of the beam should readily collide. Such a compression-tension asymmetry would impart a constrained flexibility in tessellated cartilage that could also play a role in the tissue's ability to resist damage. In general, the combination of a stiff outer cortex and a soft inner core will tend to ensure that higher stresses are concentrated more safely in the stiffer cortical/mineralized tissue rather than the softer core/unmineralized tissue [41, 61, 62]. This is true, even if the cortex is continuous rather than tessellated, as was simulated in Finite Element models of the jaws of two large shark species subjected to biologically-relevant bite forces [41].

Tessellating the cortex, however, serves additional functions, such as protecting the mineralized tissue from fracture on the tension side of the skeleton by localizing tensile stresses in the intertesseral joint fibers rather than in tesserae. At the same time, the compressive stiffness of tesserae should shift the skeleton's neutral axis of bending closer to the compressive side of the skeleton, concentrating potentially damaging compressive stresses in the tessellated layer rather than the unmineralized cartilage [61, 62]. In this way, the tessellation can manage bending loads and increase resistance to damage by distributing the highest stresses to the tissues and loading regimes best able to bear them. Stresses may also be mitigated by the properties of the unmineralized cartilage itself, which Wroe et al. [49] showed would tend to result in considerably lower stresses and higher strains than simulated shark jaws made of bone and subjected to the same bite forces (Fig. 11.12). The hypothesized stress-management behavior of tessellated cartilage may therefore serve a protective function, in a skeletal tissue that apparently cannot heal [4, 29, 38, 57], although it is surely cyclically loaded a massive number of times over an animal's lifetime during swimming and feeding behaviors.

Most models of tessellated cartilage have focused largely on the mechanical result of combining soft and hard tissues; the geometry of the tessellation—the distribution of shapes and sizes of tesserae—surely also plays an important role in the mechanics of the skeleton, yet this has hardly been investigated. Tesserae are typically polygonal in shape and apparently predominantly hexagonal, but have been observed to vary in the regularity of their form and range from squares to twelve sided polygons ([4, 39, 40, 63]; Dean, pers. obs.). Analytical models of 2D tiled arrays with joint and tile geometries and material properties varied in a range around those of tesserae, indicate

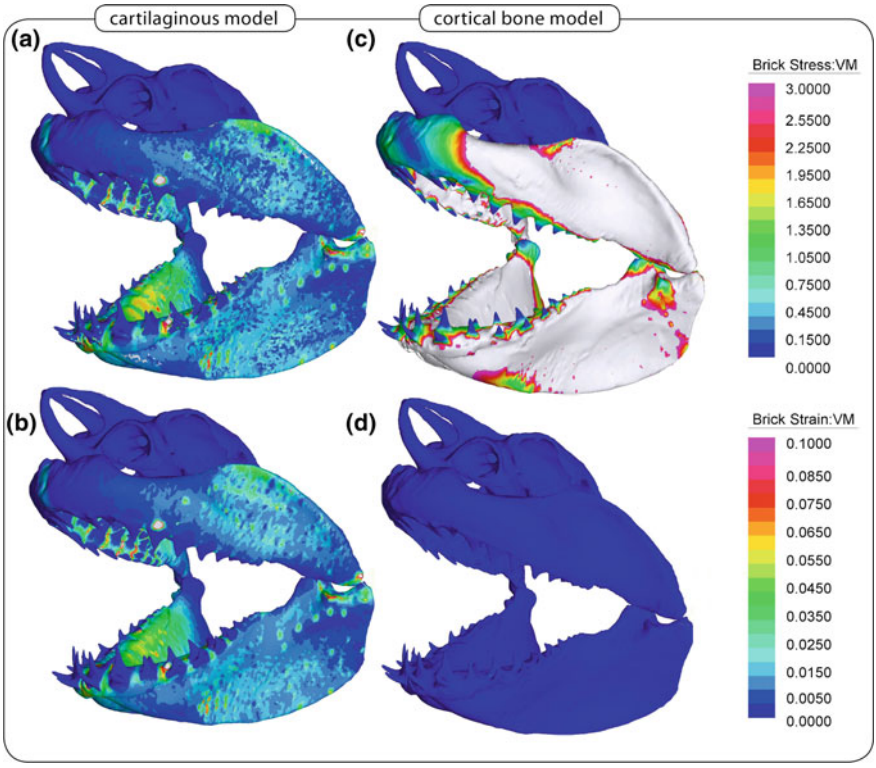

Fig. 11.12 Simulation of feeding mechanics in white shark jaws with varying material properties. **a**, **c** Von Mises stress and **b**, **d** strain distributions for maximal bilateral bites in Finite Element simulations of jaws with tessellated cartilage properties (**a**, **b**) and cortical bone properties (**c**, **d**). Note that stress is much lower, but strain is much higher in the cartilaginous model. Modified with permission from [49], copyright John Wiley Sons, Inc.

that the stiffness of the tessellation will increase the narrower joint spaces are and the stiffer tiles are relative to their joint fibers [39] (Fig. 11.13: modified from [39]). This holds true for triangular, square and hexagonal tiles, with hexagons being most sensitive to changes in model parameters and therefore allowing for a tessellation that can be more subtly 'tuned' to specific material properties. These results demonstrate that the shape of tesserae should affect the properties of the tissue composite, yet the performance of more complicated, bio-realistic tessellations (e.g. three-dimensional and/or less uniform tilings) remains to be investigated.

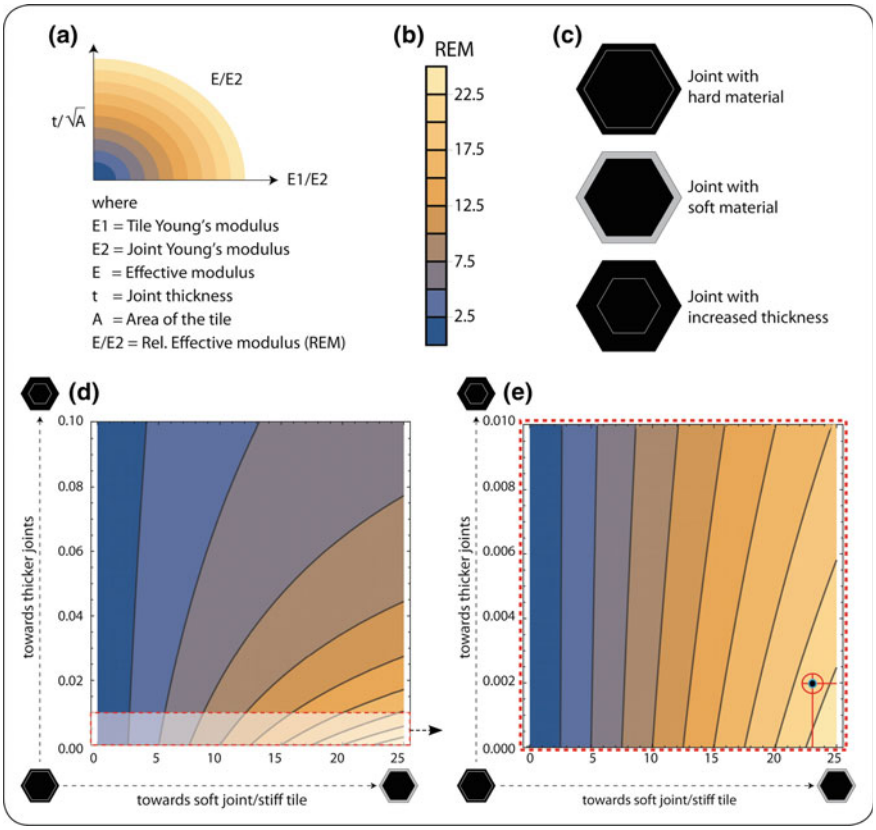

Fig. 11.13 The relative effective modulus (REM) of tessellated cartilage-inspired hexagonal tilings as a function of morphology and material properties. **a–c** Variables varied in analytical simulations of hexagonal tessellations with intervening joint material under in-plane loading. **d**, **e** Simulations show that a decrease in joint thickness (decreasing y-axis value) and an increase in the stiffness of tiles relative to joints (increasing x-axis value) results in a stiffer composite material. **e** Zoomed in view of the range of biologically relevant x- and y-axis values from **d**; structural and material properties for round stingray (*U. halleri*) tesserae are marked with red lines in the bottom right. Modified with permission from [39], copyright 2017 Elsevier

11.4 Conclusions

Although mammalian bone is commonly considered the paradigmatic vertebrate skeletal tissue, there are 'many other fish in the sea': anosteocytic and osteocytic fish bone and elasmobranch tessellated cartilage are two of Nature's skeletal design alternatives, offering valuable fodder for wider investigations on the interplay of form and function in mineralized biological materials. These tissues also present largely untapped opportunities for exploring the mechanical effects of alternate structuring in tissues with otherwise similar composition. Clearly, the distinct geometric arrange-

ments of soft and hard tissues in fish bone and tessellated cartilage have profound mechanical effects, resulting in impressive combinations of toughness and stiffness (fish bone) or stiffness and damping/flexibility (tessellated cartilage) (Fig. 11.1). Furthermore, some structural aspects of these tissues can be approximated by simple geometries (e.g. tesserae as polygonal tiles; [39]), making them particularly amenable for modeling explorations of the parameter space of biological designs (e.g. why some morphologies have evolved and not others). Although fish bone and tessellated cartilage are far less studied than mammalian skeletal tissues, they are well suited to a variety of investigations, particularly the links between ecology and biological materials (fishes occupy a massive diversity of aquatic habitats), the biological and mechanical effects of structural modifications (e.g. the loss of osteocytes, the tessellation of a skeletal cortex), and the design and behavior of hierarchically-organized composites.

References

1. P.C.J. Donoghue, I.J. Sansom, Origin and early evolution of vertebrate skeletonization. Microsc. Res. Tech. **59**, 352–372 (2002)
2. P.C.J. Donoghue, I.J. Sansom, J.P. Downs, Early evolution of vertebrate skeletal tissues and cellular interactions, and the canalization of skeletal development. J. Exp. Zool. Part B Mol. Dev. Evol. **306B**, 278–294 (2006)
3. K. Kawasaki, T. Suzuki, K.M. Weiss, Genetic basis for the evolution of vertebrate mineralized tissue. Proc. Natl. Acad. Sci. U. S. A. **101**, 11356–11361 (2004)
4. R. Seidel, K. Lyons, M. Blumer, P. Zaslansky, P. Fratzl, J.C. Weaver, M.N. Dean, Ultrastructural and developmental features of the tessellated endoskeleton of elasmobranchs (sharks and rays). J. Anat. **229**, 681–702 (2016)
5. J.-Y. Sire, A. Huysseune, Formation of dermal skeletal and dental tissues in fish: a comparative and evolutionary approach. Biol. Rev. Camb. Philos. Soc. **78**, 219–249 (2003)
6. J.D. Currey, Collagen and the mechanical properties of bone and calcified cartilage, in *Collagen: Structure and Mechanics, An Introduction*, ed. by P. Fratzl (Springer US, Boston, MA, 2008), pp. 397–420
7. E. Degtyar, M.J. Harrington, Y. Politi, P. Fratzl, The mechanical role of metal ions in biogenic protein-based materials. Angew. Chem. Int. Ed. **53**, 12026–12044 (2014)
8. J.D. Currey, The design of mineralised hard tissues for their mechanical functions. J. Exp. Biol. **202**, 3285–3294 (1999)
9. J.D. Currey, The structure and mechanics of bone. J. Mater. Sci. **47**, 41–54 (2011)
10. J.D. Currey, M.N. Dean, R. Shahar, Revisiting the links between bone remodelling and osteocytes: insights from across phyla. Biol. Rev. Camb. Philos. Soc. **92**, 1702–1719 (2017)
11. M.L. Moss, A.S. Posner, X-ray diffraction study of acellular teleost bone. Nature **188**, 1037–1038 (1960)
12. M.R. Urist, Calcium and phosphorus in the blood and skeleton of the Elasmobranchii, 1–24 (1961)
13. J.W. Smith, Collagen fibre patterns in mammalian bone. J. Anat. **94**, 329–344 (1960)
14. L.F. Bonewald, The amazing osteocyte. J. Bone Miner. Res. **26**, 229–238 (2011)
15. S.L. Dallas, M. Prideaux, L.F. Bonewald, The osteocyte: an endocrine cell … and more. Endocr. Rev. **34**, 658–690 (2013)
16. P.E. Witten, A. Huysseune, T. Franz-Odendaal, T. Fedak, M. Vickaryous, A. Cole, B.K. Hall, Acellular teleost bone: primitive or derived, dead or alive? Palaeontol. Assoc. Newsl. **55**, 37–41 (2004)

17. L. Cohen, M. Dean, A. Shipov, A. Atkins, E. Monsonego-Ornan, R. Shahar, Comparison of structural, architectural and mechanical aspects of cellular and acellular bone in two teleost fish. J. Exp. Biol. **215**, 1983–1993 (2012)
18. A. Atkins, M.N. Dean, M.L. Habegger, P.J. Motta, L. Ofer, F. Repp, A. Shipov, S. Weiner, J.D. Currey, R. Shahar, Remodeling in bone without osteocytes: billfish challenge bone structure-function paradigms. Proc. Natl. Acad. Sci. U. S. A. **111**, 16047–16052 (2014)
19. G.S. Helfman, B.B. Collette, D.E. Facey, B.W. Bowen, *The Diversity of Fishes: Biology* (Wiley-Blackwell, 2009)
20. R. Shahar, C. Lukas, S. Papo, J.W.C. Dunlop, R. Weinkamer, Characterization of the spatial arrangement of secondary osteons in the diaphysis of equine and canine long bones. Anat. Rec. **294**, 1093–1102 (2011)
21. A. Atkins, N. Reznikov, L. Ofer, A. Masic, S. Weiner, R. Shahar, The three-dimensional structure of anosteocytic lamellated bone of fish. Acta Biomater. **13**, 311–323 (2015)
22. N. Reznikov, R. Shahar, S. Weiner, Bone hierarchical structure in three dimensions. Acta Biomater. **10**, 3815–3826 (2014)
23. L.B. Halstead, Calcified tissues in the earliest vertebrates. Calcif. Tissue Int. **3**, 107–124 (1969)
24. D.R. Hughes, J.R. Bassett, L.A. Moffat, Histological identification of osteocytes in the allegedly acellular bone of the sea breams *Acanthopagrus australis*, *Pagrus auratus* and *Rhabdosargus sarba* (Sparidae, Perciformes, Teleostei). Anat. Embryol. **190**, 163–179 (1994)
25. A. Kölliker, On the different types in the microscopic structure of the skeleton of osseous fishes (1857)
26. M.L. Moss, Studies of the acellular bone of teleost fish. Cells Tissues Organs **46**, 343–362 (1961)
27. J.Y. Sire, F.J. Meunier, The canaliculi of Williamson in holostean bone (Osteichthyes, Actinopterygii): a structural and ultrastructural study. Acta Zool. **75**, 235–247 (1994)
28. T. Ørvig, Histologic studies of placoderms and fossil elasmobranchs, 1–152 (1950)
29. D.E. Ashhurst, The cartilaginous skeleton of an elasmobranch fish does not heal. Matrix Biol. **23**, 15–22 (2004)
30. B.K. Hall, *Bones and Cartilage*, 2nd edn. (Academic Press, 2014)
31. M.N. Dean, C.G. Mull, S.N. Gorb, A.P. Summers, Ontogeny of the tessellated skeleton: insight from the skeletal growth of the round stingray *Urobatis halleri*. J. Anat. **215**, 227–239 (2009)
32. N.E. Kemp, S.K. Westin, Ultrastructure of calcified cartilage in the endoskeletal tesserae of sharks. J. Morphol. **160**, 75–101 (1979)
33. R. Seidel, M.J.F. Blumer, E.J. Pechriggl, K. Lyons, B.K. Hall, P. Fratzl, J.C. Weaver, M.N. Dean, Calcified cartilage or bone? Collagens in the tessellated endoskeletons of cartilaginous fish (sharks and rays). J. Struct. Biol. (2017)
34. J.G. Maisey, The diversity of tessellated calcification in modern and extinct chondrichthyans. Rev. Paléobiol. Genève **32**, 355–371 (2013)
35. L.J. Macesic, A.P. Summers, Flexural stiffness and composition of the batoid propterygium as predictors of punting ability. J. Exp. Biol. **215**, 2003–2012 (2012)
36. J.G. Clement, Re-examination of the fine structure of endoskeletal mineralization in chondrichthyans: implications for growth, ageing and calcium homeostasis. Aust. J. Mar. Freshw. Res. **43**, 157–181 (1992)
37. S. Enault, D.N. Muñoz, W.T.A.F. Silva, V. Borday-Birraux, M. Bonade, S. Oulion, S. Ventéo, S. Marcellini, M. Debiais-Thibaud, Molecular footprinting of skeletal tissues in the catshark *Scyliorhinus canicula* and the clawed frog *Xenopus tropicalis* identifies conserved and derived features of vertebrate calcification. Front. Genet. **6**, 3133–3144 (2015)
38. R. Seidel, M. Blumer, P. Zaslansky, D. Knötel, D.R. Huber, J.C. Weaver, P. Fratzl, S. Omelon, L. Bertinetti, M.N. Dean, Ultrastructural, material and crystallographic description of endophytic masses; a possible damage response in shark and ray tessellated calcified cartilage. J. Struct. Biol. **198**, 5–18 (2017)
39. A.K. Jayasankar, R. Seidel, J. Naumann, L. Guiducci, A. Hosny, P. Fratzl, J.C. Weaver, J.W.C. Dunlop, M.N. Dean, Mechanical behavior of idealized, stingray-skeleton-inspired tiled composites as a function of geometry and material properties. J. Mech. Behav. Biomed. Mater. **73**, 1–35 (2017)

40. M.N. Dean, R. Seidel, D. Knoetel, K. Lyons, D. Baum, J.C. Weaver, P. Fratzl, To build a shark-3D tiling laws of tessellated cartilage. Integr. Comp. Biol. **56**, E50 (2016)
41. T.L. Ferrara, P. Clausen, D.R. Huber, C.R. McHenry, V. Peddemors, S. Wroe, Mechanics of biting in great white and sandtiger sharks. J. Biomech. **44**, 430–435 (2011)
42. X. Liu, M.N. Dean, H. Youssefpour, A.P. Summers, J.C. Earthman, Stress relaxation behavior of tessellated cartilage from the jaws of blue sharks. J. Mech. Behav. Biomed. Mater. **29**, 68–80 (2014)
43. M.E. Porter, J.L. Beltran, S.M. Kajiura, T.J. Koob, A.P. Summers, Stiffness without mineral: material properties and biochemical components of jaws and chondrocrania in the Elasmobranchii (sharks, skates, and rays). PeerJ **1**, e47v1 (2013)
44. R. Martini, Y. Balit, F. Barthelat, A comparative study of bio-inspired protective scales using 3D printing and mechanical testing. Acta Biomater. **55**, 360–372 (2017)
45. S.R. Fahle, J.C. Thomason, Measurement of jaw viscoelasticity in newborn and adult lesser spotted dogfish *Scyliorhinus canicula* (L., 1758). J. Fish Biol. **72**, 1553–1557 (2008)
46. M. Egerbacher, M. Helmreich, E. Mayrhofer, P. Böck, Mineralisation of the hyaline cartilage in the small-spotted dogfish *Scyliorhinus canicula* L. *Scripta Medica (BRNO)* (2006)
47. T.L. Ferrara, P. Boughton, E. Slavich, S. Wroe, A novel method for single sample multi-axial nanoindentation of hydrated heterogeneous tissues based on testing great white shark jaws. PLoS ONE **8**, e81196 (2013)
48. S. Applegate, A survey of shark hard parts. In *Sharks, Skates and Rays* (1967), pp. 37–67
49. S. Wroe, D.R. Huber, M. Lowry, C. McHenry, K. Moreno, P. Clausen, T.L. Ferrara, E. Cunningham, M.N. Dean, A.P. Summers, Three-dimensional computer analysis of white shark jaw mechanics: how hard can a great white bite? J. Zool. **276**, 336–342 (2008)
50. M.N. Dean, A.P. Summers, Mineralized cartilage in the skeleton of chondrichthyan fishes. Zoology **109**, 164–168 (2006)
51. A.P. Summers, Stiffening the stingray skeleton—an investigation of durophagy in myliobatid stingrays (Chondrichthyes, Batoidea, Myliobatidae). J. Morphol. **243**, 113–126 (2000)
52. A.P. Summers, R.A. Ketcham, T. Rowe, Structure and function of the horn shark (*Heterodontus francisci*) cranium through ontogeny: development of a hard prey specialist. J. Morphol. **260**, 1–12 (2004)
53. M.N. Dean, D.R. Huber, H.A. Nance, Functional morphology of jaw trabeculation in the lesser electric ray *Narcine brasiliensis*, with comments on the evolution of structural support in the Batoidea. J. Morphol. **267**, 1137–1146 (2006)
54. M.A. Kolmann, S.B. Crofts, M.N. Dean, A.P. Summers, N.R. Lovejoy, Morphology does not predict performance: jaw curvature and prey crushing in durophagous stingrays. J. Exp. Biol. **218**, 3941–3949 (2015)
55. R. Seidel, M. Blumer, E.-J. Pechriggl, K. Lyons, B.K. Hall, P. Fratzl, J.C. Weaver, M.N. Dean, Calcified cartilage or bone? Collagens in the tessellated endoskeletons of cartilaginous fish (sharks and rays). J. Struct. Biol. **200**, 1–35 (2017)
56. J.P. Balaban, A.P. Summers, C.A. Wilga, Mechanical properties of the hyomandibula in four shark species. J. Exp. Zool. Part A Ecol. Genet. Physiol. **323**, 1–9 (2014)
57. M.N. Dean, J.J. Bizzarro, B. Clark, C.J. Underwood, Z. Johanson, Large batoid fishes frequently consume stingrays despite skeletal damage. R. Soc. Open Sci. **4**, 170674–11 (2017)
58. C.A.D. Wilga, S.E. Diniz, P.R. Steele, J. Sudario-Cook, E.R. Dumont, L.A. Ferry, Ontogeny of feeding mechanics in smoothhound sharks: morphology and cartilage stiffness. Integr. Comp. Biol. **56**, 442–448 (2016)
59. G. Dingerkus, B. Seret, Multiple prismatic calcium phosphate layers in the jaws of present-day sharks (Chondrichthyes; Selachii). Experientia **47**, 38–40 (1991)
60. W. Huang, W. Hongjamrassilp, J.-Y. Jung, P.A. Hastings, V.A. Lubarda, J. McKittrick, Structure and mechanical implications of the pectoral fin skeleton in the Longnose Skate (Chondrichthyes, Batoidea). Acta Biomater. **51**, 393–407 (2017)
61. P. Fratzl, O. Kolednik, F.D. Fischer, M.N. Dean, The mechanics of tessellations—bioinspired strategies for fracture resistance. Chemical Society Reviews **45**, 252–267 (2016)

62. X. Liu, M.N. Dean, A.P. Summers, J.C. Earthman, Composite model of the shark's skeleton in bending: a novel architecture for biomimetic design of functional compression bias. Mater. Sci. Eng. C **30**, 1077–1084 (2010)
63. M.N. Dean, J.T. Schaefer, Patterns of growth and mineralization in elasmobranch cartilage. Faseb J. **19**, A247–A247 (2005)
64. L.A. Jawad, Hyperostosis in three fish species collected from the Sea of Oman. Anat. Rec. **296**, 1145–1147 (2013)